pISSN 1229-3008 eISSN 2287-6251
Progress in Superconductivity and Cryogenics
Vol.18, No.2, (2016), pp.30~36 http://dx.doi.org/10.9714/psac.2016.18.2.030

Study on magnetic field mapping within cylindrical center volume of general magnet

Li Huang and Sangjin Lee*

Uiduk University, Gyeongju, Republic of Korea

(Received 8 June 2016; revised or reviewed 27 June 2016; accepted 28 June 2016)

Abstract

For the magnetic field analysis or design, it is important to know the behavior of the magnetic field in an interesting space. Magnetic field mapping becomes a useful tool for the study of magnetic field. In this paper, a numerical way for mapping the magnetic field within the cylindrical center volume of magnet is presented, based on the solution of the Laplace's equation in the cylindrical coordinate system. The expression of the magnetic field can be obtained by the magnetic flux density, which measured in the mapped volume. According to the form of the expression, the measurement points are arranged with the parallel cylindrical line (PCL) method. As example, the magnetic flux density generated by an electron cyclotron resonance ion source (ECRIS) magnet and a quadrupole magnet were mapped using the PCL method, respectively. The mapping results show the PCL arrangement method is feasible and convenience to map the magnetic field within a cylindrical center volume generated by the general magnet.

Keywords: cylindrical volume, Laplace's equation, magnetic field mapping, parallel cylindrical line

1. INTRODUCTION

In the application of magnet, it is important to obtain accurate information about the magnetic field [1-2]. Normally a map of the magnetic field distribution is frequently needed to guarantee the characteristics of the magnetic field.

In order to map the field, the easy and direct way is to measure the magnetic field at each point in the interesting volume. However the measurement time will be unendurable due the large number of measurement points. The indirect way for the mapping the magnetic field is to use the mathematic tool. Considering the magnetic field should satisfy the Maxwell's equation, the field in the magnet can be described by some mathematic functions. Applying measurement data to fit these mathematic functions, the magnetic field in the whole volume can be calculated.

According to the different mathematical equations, some indirect mapping methods have been developed in practice. H. Takeda introduced a numerical method to map the field from 2D field measurements of the surface of a cylinder [3]. This method is flexible, but cannot be applied to the solenoidal field. P. Vernin described a method to map the residual magnetic flux, which is the difference between the 3D model and the measured flux [4]. This method is powerful, but it is complex to build a 3D model of magnet, when the magnet is unknown. In order to obtain a mapping method for the various types of magnetic field, Lorentzian curves are employed to fit the field in the mapping method.

In this paper, according to the solution of the Laplace's equation in the cylindrical coordinate system, a PCL arrangement method for the magnetic field mapping was presented. The theorem of the PCL arrangement method was described in section 2. Using the PCL arrangement method, the magnetic flux density in the center of an ECRIS magnet and a quadrupole magnet were mapped in section 3, respectively. As shown in the mapping results, the PCL arrangement method is feasible and convenient to map the magnetic field within a cylindrical volume in the center of magnet. And the PCL arrangement method can be widely applied in the magnetic field generated by various types of magnet.

*Corresponding author: sjlee@uu.ac.kr

2. THEOREM FOR MAPPING

2.1. Solution of Laplace's Equation

According to the Maxwell's equations, the magnetic scalar potential V in a static magnetic field should be satisfied the Laplace's equation when there are no current sources or current sinks in the volume. In the cylindrical coordinate (ρ, φ, z), where ρ is the radial distance, φ is the azimuthal angle, and z is the height, the fundamental solutions of the Laplace's equation are the Bessel function $J_n(m\rho)$, $Y_n(m\rho)$, trigonometric functions $\cos n\varphi$, $\sin n\varphi$, and exponential functions $e^{\pm mz}$, respectively. Here, n and m are constants introduced in the process of separation of variables method. The general solution of the Laplace's equation in the cylindrical coordinate system is their linear combination.

For the magnetic scalar potential V in the center volume, the Bessel function can be expanded as a power series of ρ, the linear combination of exponential functions are denoted as functions $A_{n,m}(z)$ and

$B_{n,m}(z)$. And the magnetic scalar potential V can be written as [5]

$$V(\rho,\varphi,z)=\sum_{n=0}^{\infty}\sum_{m=0}^{\infty}\left(\frac{\rho}{\rho_0}\right)^{n+2m}\rho_0^{2m}\left[A_{n,m}(z)\sin(n\varphi)+B_{n,m}(z)\cos(n\varphi)\right] \quad (1)$$

where ρ_0 is the reference radius.

Then the magnetic flux density can be calculated by

$$B_{\rho}=\sum_{n=0}^{\infty}\sum_{m=0}^{\infty}\left(\frac{\rho}{\rho_0}\right)^{n+2m-1}(n+2m)\rho_0^{2m-1}\left[A_{n,m}(z)\sin(n\varphi)+B_{n,m}(z)\cos(n\varphi)\right] \quad (2)$$

$$B_{\varphi}=\sum_{n=0}^{\infty}\sum_{m=0}^{\infty}\left(\frac{\rho}{\rho_0}\right)^{n+2m-1}n\rho_0^{2m-1}\left[A_{n,m}(z)\cos(n\varphi)-B_{n,m}(z)\sin(n\varphi)\right] \quad (3)$$

$$B_{z}=\sum_{n=0}^{\infty}\sum_{m=0}^{\infty}\left(\frac{\rho}{\rho_0}\right)^{n+2m}\rho_0^{2m}\left[\frac{dA_{n,m}(z)}{dz}\sin(n\varphi)+\frac{dB_{n,m}(z)}{dz}\cos(n\varphi)\right] \quad (4)$$

In order to apply these equations to calculate the components of the magnetic flux density, we need to know the functions $A_{n,m}(z)$ and $B_{n,m}(z)$. Considering the magnetic scalar potential V should satisfy the Laplace's equation, substituting (1) into the Laplace's equation, we can get

$$A_{n,m}(z)=-\frac{1}{4m(n+m)}\frac{d^2}{dz^2}A_{n,m-1}(z) \quad (5)$$

and

$$B_{n,m}(z)=-\frac{1}{4m(n+m)}\frac{d^2}{dz^2}B_{n,m-1}(z) \quad (6)$$

According to (5) and (6), the functions $A_{n,m}(z)$ and $B_{n,m}(z)$ can be calculated by

$$A_{n,m}(z)=C_{n,m}\frac{d^{2m}}{dz^{2m}}A_{n,0}(z) \quad (7)$$

and

$$B_{n,m}(z)=C_{n,m}\frac{d^{2m}}{dz^{2m}}B_{n,0}(z) \quad (8)$$

where $C_{n,m}=\frac{(-1)^m n!}{4^m m!(n+m)!}$.

The magnetic field mapping is to find these unknown function $A_{n,0}(z)$ and $B_{n,0}(z)$.

2.2. Lorentzian Curve

In order to obtain the unknown functions $A_{n,0}(z)$ and $B_{n,0}(z)$, the form of these functions should be determined at first. In the magnetic scalar potential V, the unknown functions $A_{n,0}(z)$ and $B_{n,0}(z)$ are continuous in z and have an infinite order derivative. Furthermore, the value of functions $A_{n,0}(z)$ and $B_{n,0}(z)$ approach to zeros when z is infinite. Due to the shape of Lorentzian curve, the unknown functions $A_{n,0}(z)$ and $B_{n,0}(z)$ can be approximated by the sum of Lorentzian curves. The Lorentzian curve $f(x)$ can be expressed by

$$f(x)=\frac{a}{(x-x_0)^2+L^2} \quad (9)$$

where x_0 is the center of curve, a and L determine the magnitude and the width of the curve.

Assume there are N curves in the mapping procedure, the unknown functions $A_{n,0}(z)$ and $B_{n,0}(z)$ can be approximated by

$$A_{n,0}(z)=\sum_{j=1}^{N}\frac{a_{nj}}{(z-z_{nj})^2+L_n^2} \quad (10)$$

and

$$B_{n,0}(z)=\sum_{j=1}^{N}\frac{b_{nj}}{(z-z_{nj})^2+L_n^2} \quad (11)$$

where a_{nj} and b_{nj} are the unknown constants, z_{nj} can be determined by the height of measurement points, L_n is a constant. The value of z_{nj} and L_n can be optimized by the measurement data.

Considering the components of magnetic flux density are the sum of $\sin n\varphi$ and $\cos n\varphi$, the coefficients of $\sin n\varphi$ and $\cos n\varphi$ can be obtained by the discrete Fourier transform (DFT). Then for $\sin n\varphi$ terms in the component B_{ρ}, we can get

$$B_{\rho,n}=\sum_{m=0}^{\infty}\left(\frac{\rho}{\rho_0}\right)^{n+2m-1}(n+2m)C_{n,m}\rho_0^{2m-1}\frac{d^{2m}}{dz^{2m}}\left(\sum_{j=1}^{N}\frac{a_{nj}}{(z-z_{nj})^2+L_n^2}\right) \quad (12)$$

If the N coefficients have been obtained at different height z, using (12), a linear equations set for a_{nj} can be obtained, and written as the matrix form

$$\boldsymbol{B}_{\rho,n}=\boldsymbol{M}_n\boldsymbol{a}_n \quad (13)$$

where $\boldsymbol{B}_{\rho,n}$ is the vector of the coefficients of $\sin n\varphi$ term according to the DFT, $\boldsymbol{M}_n$ is the matrix whose components are calculated by (12), and $\boldsymbol{a}_n$ is the vector of the unknown constants a_{nj}.

Using the coefficients of $\cos n\varphi$ term, we can solve the unknown constants b_{nj}. Once all of a_{nj} and b_{nj} are known, the component B_{ρ} can be calculated by (2). Similarly, we can calculate the components B_{φ} and B_z.

2.3. PCL Arrangement Method

In the mapping procedure, the measurement points can be arranged along several circles, which are in parallel with the plane $z=0$. The trajectories of probes are several PCLs in the center volume of magnet. And the measurement points are distributed uniformly on each circle. This arrangement method of measurement points is named by the PCL arrangement method and shown in Fig. 1. And the parameters of the PCL arrangement method are listed in Table I.

The process of the magnetic field mapping can be described in Fig. 2. According to the PCL arrangement

method, the components of the magnetic field are measured in the center of the magnet. Then using the Fourier transform with respect to φ, the coefficients of trigonometric function of $n\varphi$ in (2), (3), and (4) can be obtained. And these coefficients can be viewed as the functions of (ρ, z) as shown in (12). The Lorentzian curves are employed to fit these functions. Considering the values of ρ and z are known from the parameters of the PCL arrangement method, the unknown constants a_{nj} and b_{nj} can be solved. After that then substitute them into (10) and (11), we can get the unknown function $A_{n,0}(z)$ and $B_{n,0}(z)$. At last, the components of magnetic field at other points can be calculated using (2), (3), and (4).

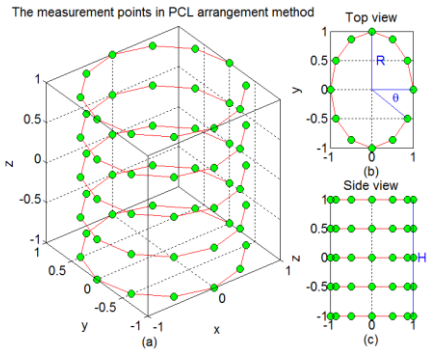

Fig. 1. The measurement points in the PCL arrangement method. (a) position of measurement points (b) top view (c) side view.

TABLE I
PARAMETERS OF THE PCL ARRANGEMENT METHOD.

Parameter	Description
R	Radius of cylindrical surface
H	Height of cylindrical surface
φ	Azimuthal angle
N_a	Number of points on each circle
N_h	Number of circles
r_0	Reference radius

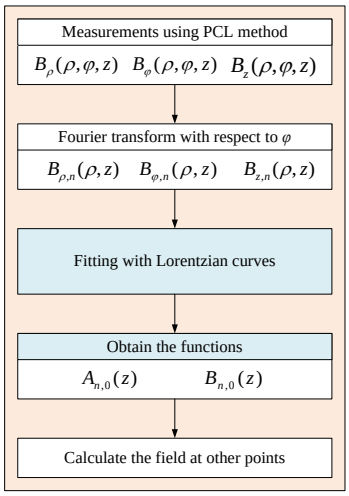

Fig. 2. The process of the field mapping using the PCL arrangement method.

3. CASE STUDY

3.1. ECRIS Magnet

The ECRIS is used for providing intense highly charged ion beams to the linear accelerator. The structure of ECRIS magnet is composed of four axial coils and six radial coils. The configuration of the axial coils consists of four coaxial solenoids with different dimensions and currents. And the six radial coils is in a sextupole configuration. The sextupole is placed inside the solenoids (sextupole-in-solenoid geometry) as shown in Fig. 3. The magnet system provides an axial magnetic field from four solenoid coils and a radial magnetic field from sextupole magnet to confine the ECR plasma stream. The designed parameters of coils in the magnet system have been listed in Table II.

In this case study, the magnetic field generated by the solenoid was simulated by a "*rzBI*" program with high accuracy [6]. Considering the magnetic field generated by the straight wire can be calculated by the closed-form expression, the magnetic field generated by the sextupole magnet was simulated by six identical current loops as shown in Fig. 4. Then the magnetic field can be calculated using the superposition of fields generated by straight lines and the solenoid. In the case study, it is not necessary to use the FEM (finite element method) in the magnetic field calculation.

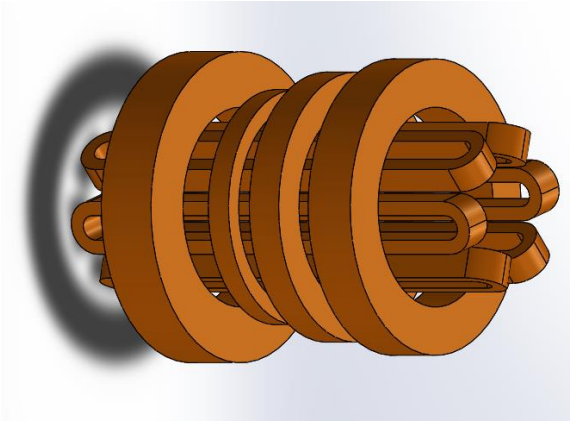

Fig. 3. Structure of ECRIS magnet which is composed of four solenoids and a sextupole magnet.

TABLE II
PARAMETERS OF COILS IN ECRIS MAGNET.

	Unit	Solenoid Coils				Sextupole Coils
		1	2	3	4	
Axial position of center	mm	-250	-73	67	250	
Inner radius	mm	205	205	205	205	100
Depth	mm	114	36	72	99	65
Width	mm	125	51	74	106	41
Turns/coil		9965	1283	3725	7338	1863
Current	A	-169	154	148	-139	250

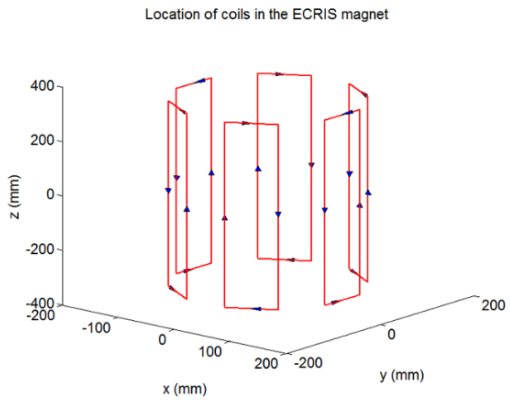

Fig. 4. Six identical current loops for the simulation of sextupole magnet in the ECRIS magnet.

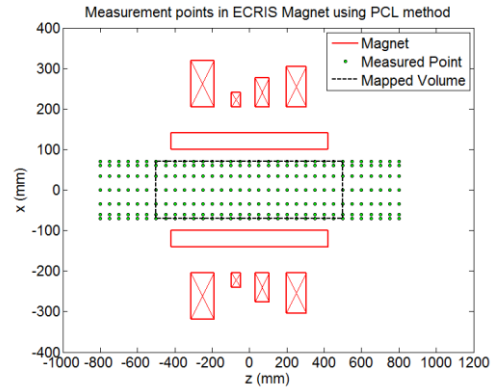

Fig. 5. The position of the measurement points and the mapped volume in the ECRIS magnet using PCL method.

TABLE III
PARAMETERS OF PCL METHOD FOR MAPPING.

Description	Symbol	Value
Radius	R	70 mm
Azimuthal Angle	φ	5.625°
Height	H	1600 mm
Number of points on each circle	N_a	64
Number of circle	N_h	161
Distance between circles	D_c	10 mm
Reference Radius	r_0	70 mm

Assume the mapped volume is a height 1000 mm and radius 70 mm cylindrical volume in the center of ECRIS magnet. The measurement points using the PCL arrangement method have been shown in Fig. 5, and the parameters of the PCL arrangement method are listed in Table III.

Using to the PCL arrangement method, the components of magnetic flux density at the measurement points in the center of the ECRIS magnet can be obtained. According to the DFT, the maximum value of n in (2), (3), and (4) can be calculated by $N_a/2$. Considering ECRIS magnet has a six-fold symmetry, the components of the Fourier series have greater values when n is 3, 9, 15, and so on. In the mapping procedure, the components of the Fourier series, which magnitude is too small, can be neglected.

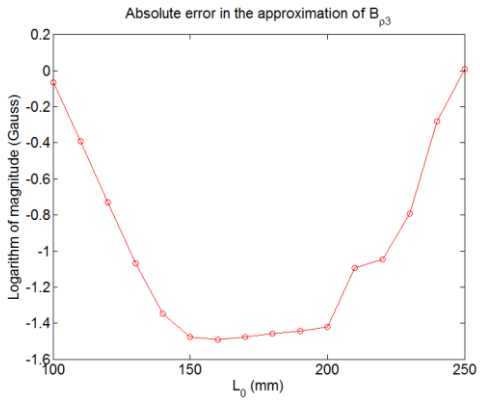

Fig. 6. Absolute error in the calculation of $B_{\rho 3}$ changes with the value of L_3.

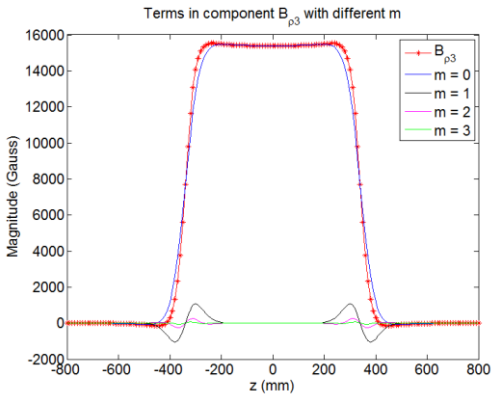

Fig. 7. Terms in the calculation of component $B_{\rho 3}$.

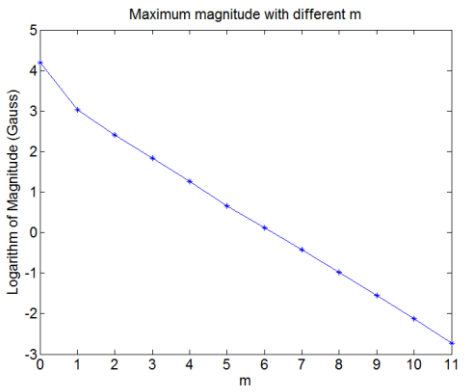

Fig. 8. Maximum magnitude of terms in the calculation of component $B_{\rho 3}$.

The value of L_n can be optimized by the measurement data. Illustrated by the case of $n = 3$ term in the component B_ρ, the error in the mapping procedure has been calculated as shown in Fig. 6. When L_3 is 150 mm, the error in the calculation can get a minimum value.

According to (12), the component $B_{\rho 3}$ can be calculated by the sum of high order derivatives of Lorentzian curves. The magnitudes of the terms in (12) will reduce with the increasing of m as shown in Fig. 7 and the maximum value in each m have been plotted in Fig. 8. When m is up to 10, the absolute error in the calculation of $B_{\rho 3}$ will less than 0.01 Gauss.

Once all of $\sin n\varphi$ and $\cos n\varphi$ terms in the component B_ρ have been obtained, using (2), the component B_ρ at any point in the mapped volume can be calculated. In the same way, the components B_φ and B_z in the volume can be obtained. The absolute errors in the components B_ρ, B_φ, and B_z have been shown in Fig. 9. The mapping result of B_z is worse than the others, however, the absolute error in the mapping result is almost less than 0.1 Gauss. Considering the range of field strength instrument using the Hall effect is from 0.1 mT to 3×10^4 mT, the mapping result is acceptable.

Using the HCL arrangement method introduced in the reference [7-8], the absolute errors of each components in the mapped volume have been shown in Fig. 10. Compared with the mapping result using the HCL arrangement method, the radial component B_ρ and the azimuthal components B_φ mapped using the PCL arrangement method are better than the mapping results using the HCL arrangement method. And the mapping result using the HCL arrangement method becomes worse at the both end of the mapped volume.

The distribution of the components of the magnetic field in the partial of the mapped volume have been shown in Fig. 11.

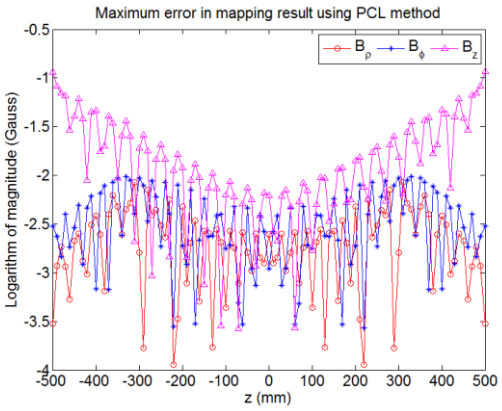

Fig. 9. Absolute error in the components of magnetic flux density mapping in the ECRIS magnet using PCL method.

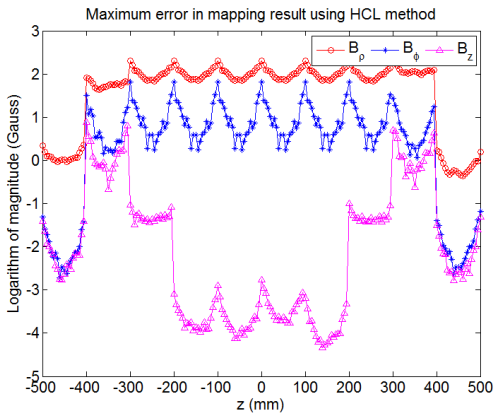

Fig. 10. Absolute error in the magnetic flux density mapping in the ECRIS magnet using HCL method.

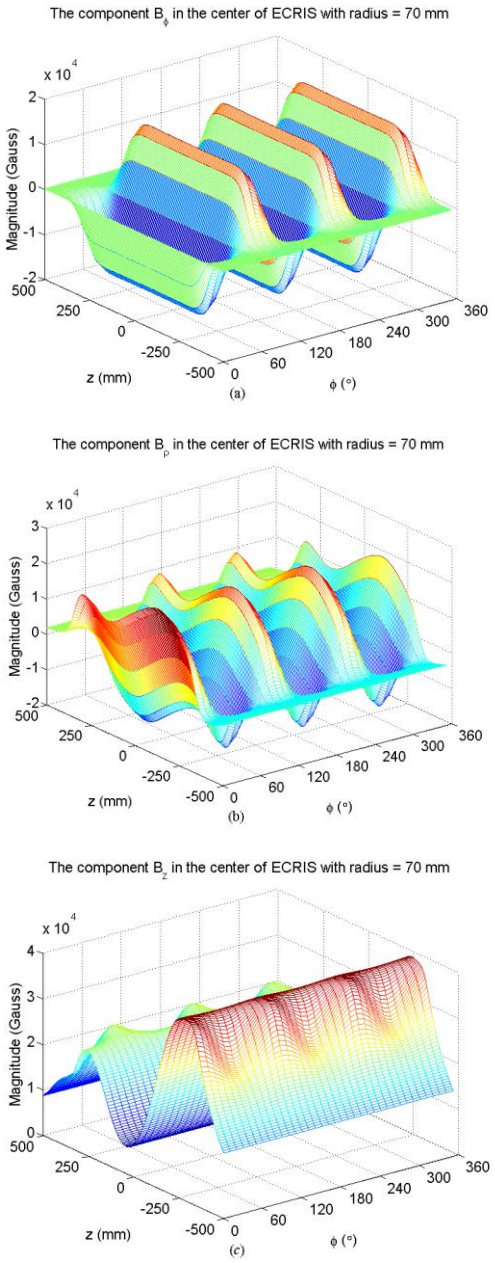

Fig. 11. The distribution of the components in the magnetic flux density in the center of ECRIS magnet with radius = 70 mm. (a) the component B_φ (b) the component B_ρ (c) the component B_z.

3.2. Quadrupole Magnet

Quadrupole magnet is useful in the particle beam focusing because the magnitude of the magnetic field generated by the quadrupole magnet grows rapidly with the radial distance from the longitudinal axis. In the case study, the quadrupole magnet is simulated by four identity current loops as shown in Fig. 12 and the parameters of these current loops are listed in Table IV.

Assume the mapped volume is a height 1000 mm and radius 170 mm cylindrical volume in the center of the quadrupole magnet. The measurement points using the PCL arrangement method have been shown in Fig. 13, and the parameters of the PCL arrangement method are listed in Table V.

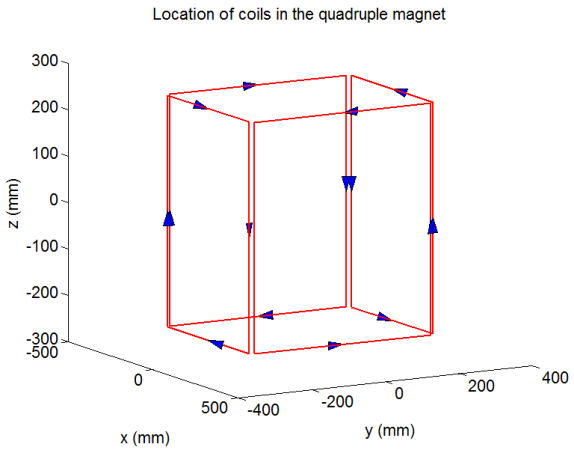

Fig. 12. Four identical current loops for the simulation of the quadrupole magnet (in order to show four loops, there are some gaps between them).

TABLE IV
PARAMETERS OF CURRENT LOOPS FOR QUADRUPOLE MAGNET.

Description	Value
Height	500 mm
Length	500 mm
Distance between opposite loops	500 mm
Operating current	300 kA

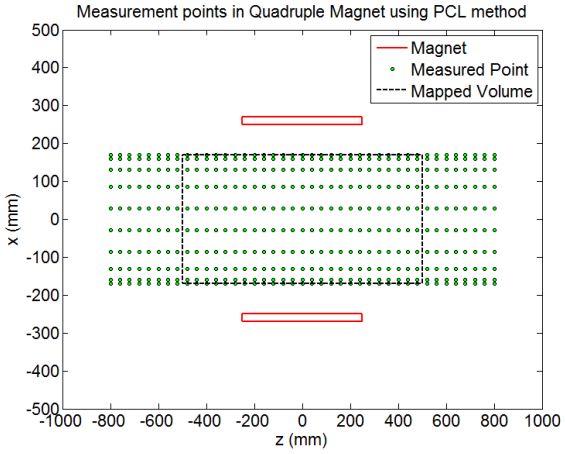

Fig. 13. The position of the measurement points and the mapped volume in the quadrupole magnet

TABLE V
PARAMETERS OF PCL METHOD FOR MAPPING

Description	Symbol	Value
Radius	R	170 mm
Azimuthal Angle	φ	10°
Height	H	1600 mm
Number of points on each circle	N_a	36
Number of circle	N_h	161
Distance between circles	D_c	10 mm
Reference Radius	r_0	170 mm

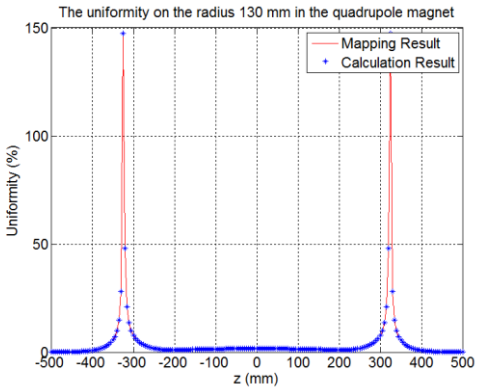

Fig. 14. The uniformity in the quadrupole magnet on the surface of the cylinder with 130 mm radius

In the center of the quadrupole magnet, the components of the magnetic field is a four-fold symmetry. The components of the Fourier series have greater values when n is 2, 6, 10, and so on. Define the uniformity of the field in the quadrupole magnet is

$$U = \frac{|B_{\rho 6}(z)|}{|B_{\rho 2}(z)|} \times 100\% \tag{14}$$

where $B_{\rho 6}(z)$ and $B_{\rho 2}(z)$ are the $n = 6$ term and the $n = 2$ term in the Fourier series with respect to z, respectively.

According to the mapping result and the calculation result, the uniformity on the radius 130 mm can be obtained as shown in Fig. 14. The uniformity from the mapping results is almost same as the uniformity from the calculation results from the simulation.

The mapping error is checked by the difference between the mapping result and the simulation result. The maximum absolute error on the surface of circle with respect to z have been plotted in Fig. 15. Compared with the mapping error using the Fourier transform method introduced in the reference [3], the PCL arrangement method can obtain a more accurate mapping result as shown in Fig. 16.

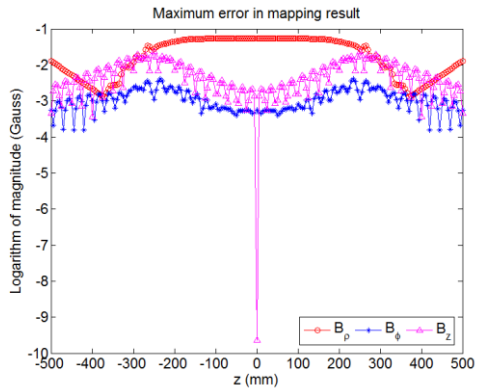

Fig. 15. Absolute error in the components of magnetic flux density mapping in the quadrupole magnet using the PCL arrangement method.

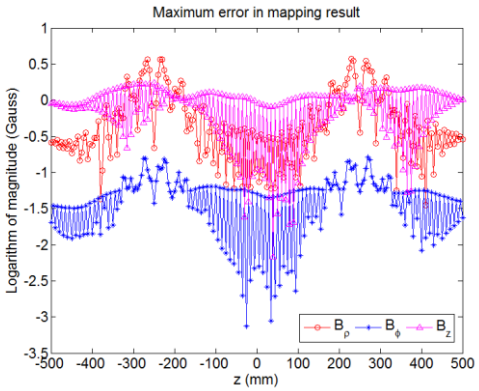

Fig. 16. The mapping error using the method from the reference [3].

4. CONCLUSION

Using the solution of the Laplace's equation in the cylindrical coordinate system, a PCL arrangement method is applied to map the magnetic field within the center volume of magnet. The method is suitable for the magnetic field mapping in a cylindrical volume, and can be widely applied in the field mapping generated by various types of magnet. The magnetic field mapping in the ECRIS magnet and the quadrupole magnet have shown that the PCL arrangement method is feasible and convenient.

REFERENCES

[1] Y. Jing *et al*., "Magnetic Field Mapping in the BESIII Solenoid," *IEEE Transactions on Applied Superconductivity*, vol. 20, no. 3, pp. 324-327, 2010.

[2] N. Tan *et al*., "Magnetic Field Mapping of the Belle Solenoid," *IEEE Transactions on Nuclear Science*, vol. 48, no. 3, pp. 900-907, 2001.

[3] H. Takeda *et al*., "Extraction of 3D field maps of magnetic multipoles from 2D surface measurements with applications to the optics calculations of the large-acceptance superconducting fragment separator BigRIPS," *Nucl. Instrum. Meth*. Part B, vol. 317, pp. 798-809, 2013.

[4] P. Vernin *et al*., "Field mapping of the Hall A high-resolution spectrometers of the Thomas Jefferson National Accelerator Facility (Jefferson Lab)," *Nucl. Instrum. Meth*. Part A, vol. 449, pp. 505-527, 2000.

[5] S. Caspi *et al*., "The Use of Harmonics in 3-D Magnetic Fields," *IEEE Transactions on Magnetics*, vol. 30, no. 4, pp. 2419-2422, 1994.

[6] L. Huang and S. Lee, "Development of a magnetic field calculation program for air-core solenoid which can control the precision of a magnetic field," *Progress in Superconductivity and Cryogenics*, vol. 16, no. 4, pp. 53-56, 2014.

[7] L. Huang and S. Lee, "Study on Magnetic Field Mapping Method in the Center Volume of the Air-Core Solenoid," *IEEE Transactions on Applied Superconductivity*, Vol. 26, Iss. 4, pp. 4900104, 2016.

[8] L. Huang and S. Lee, "A study on the effect of the condition number in the magnetic field mapping of the Air-Core solenoid," *Progress in Superconductivity and Cryogenics*, vol. 17, no. 2, pp. 31-35, 2015.

[9] J. S. Arora, *Introduction to Optimum Design*, Third Ed., Elsevier, Academic Press, 2012.